MAGIC 99-2

Constraints in using APDs in Air-Cherenkov-Telescopes for γ astronomy

M. Martinez, A. Ostankov
IFAE, Barcelona, Spain

E. Lorenz, R. Mirzoyan
MPI, Munich, Germany

Abstract

The constraints in using APDs for future air Cherenkov telescope cameras coming from the limited gain and the different electronic noise sources are discussed. Special emphasis is put into the discussion of the APDs excess noise factor. Different operational strategies are presented and possible new hardware developments are suggested.

1 Introduction

TeV gamma ray (γ) astronomy is currently in a rapid expansion. The most promising detectors are air Cherenkov telescopes (ACTs) with fine pixelized focal plane cameras. Current efforts concentrate on lowering the threshold down to $\sim$ 20 GeV where satellite detectors become insensitive due to area constraints. Fast, high quantum efficiency (QE) photosensors are the most promising element for future improvements as mirror sizes are already close to their technical limits.

Avalanche photodiodes (APD) are currently under study as a possible photodetector option for the MAGIC telescope [1] image camera[1]. The main advantage of such a photosensor is its intrinsically high quantum efficiency ($QE > 70\%$) and wide spectral range which allows to reduce the trigger threshold of the telescope an to increase the image reconstruction efficiency just above threshold. Because of the Poisson-like nature of photostatistics of shower image at the camera[2], the threshold on the trigger level should follow a simple law:

$$Threshold_{(trigger)} \sim \frac{Signal}{Noise} \sim \sqrt{N_{ph.e^-}} \sim \sqrt{QE} \qquad (1)$$

while, at the same time, the reconstruction efficiency or threshold on the image reconstruction level (off-line analysis) should follow:

$$Threshold_{(reconstruction)} \sim N_{ph.e^-} \sim QE \qquad (2)$$

This trivial statement, in which we do not take into account trigger topology and other things which may complicate these simple relations, just indicates that using detectors with the highest QE we can gain even more at the reconstruction level that at the trigger stage.

Probably the best commercially available APDs at the moment which already now can meet most of the future ACT camera needs [2] (see [1]) are

[1]This study has been carried out in connection to the proposal for the 17 m. diameter MAGIC telescope but the findings can easily be transferred to other ACTs or even air fluorescence detectors. For simplicity we refer to MAGIC as an example of an ACT.

[2]Except perhaps one of the qualities aimed, although not really a basic need of the system to cope with its physics program, which is the ability to see a single photoelectron peak for system calibration and, in addition, the capability of single photoelectron resolution.

the ones produced by the RMD Company (Radiation Monitoring Devices, Inc., Watertown, USA). The table 1 presents some important parameters for noise analysis of the RMD high gain APDs[3].

It has been advertised by RMD that such APDs with gain of 10000 at room temperature and up to 40000 at moderate (-45^{o}C) cooling, approach the ability to detect a single optical photon[4]. On the basis of results presented in their article it is difficult to make a clear conclusion about the possibility to use these devices for a future ACT camera especially taking into account that it strongly depends on the preamplifier used.

However, using as a reference the APD parameters listened in table 1 we've performed several studies to check how, in general, such devices might be used to cope with the camera needs of future ACTs. This is the main subject of this note.

2 Noise consideration for APD+Preamplifier system

In the following we assume the use of a very fast charge sensitive preamplifier with a JFET input and a shaping amplifier leading to a bandwidth B. The RMS detector shot noise current density for a bandwidth B is given by:

$$i_d/B^{1/2} = [2q(I_S M^2 F + I_{edge} + I_{bulk} M^2 F)]^{1/2}, \tag{3}$$

where q – is the electron charge, M – it the APD gain, I_S – is the signal of interest, I_{edge} – is the surface leakage current which yields conventional shot noise and I_{bulk} – is the thermally generated bulk leakage current in the semiconductor section before the amplification. This last current is amplified and together with I_S yields excess shot noise. Finally, F is the excess noise factor which, given its importance for limiting the possibility of resolving single photoelectrons in the case of the APDs, deserves a dedicated discussion which we'll present in the next section.

Given the small number of photoelectrons expected in ACTs, the description of the signal in terms of a superposition of single photolectron pulses is preferable to be considered instead of the current. According to Campbell's theorem the sum of mean square contributions of all preceding impulses equals the variance. It gives for incoming current I_{in} and amplifier with semi-gaussian shaping resulting variance $\sigma^2 = I_{in}\tau/q$, where τ is amplifier time constant.[3]

In such a case the total charge fluctuation is

$$G_{tot}^2 \approx M^2 F N_{signal} + M^2 F \frac{I_{bulk}\tau}{q} + \frac{I_{edge}\tau}{q} + C_{APD}^2 \frac{4k_B T}{1.5 g_m q^2 \tau} \tag{4}$$

The last term in this equation is the amplifier ENC where, as usual C_{APD}, T, k_B and g_m – are the detector capacitance, temperature, Boltzmann constant and transconductance of the JFET preamplifier respectively. This term is obtained usually from a more general expression[5] valid for ideal 'cusp' shaping time and field-effect devices

$$ENC_{preamp}^2 = 4k_B T C_{det}[(\frac{C_{det}}{C_{preamp'}})^{1/2} + (\frac{C_{preamp'}}{C_{det}})^{1/2}]^2 \tau_A/(1.5\tau), \tag{5}$$

here $\tau_A = C_{preamp}/g_m$ approaches the electron transit time through the the amplifier region of the transistor where parasitic capacitances and resistances are neglected. The term in brackets is a measure of the capacitance mismatch between the detector and, on the other hand, the preamp input capacitance and parasitic parallel capacitances (cables, connections,...), $C_{preamp'}$. It is clear that this term has a minimum for $C_{det} \approx C_{preamp}$ assuming matched connections.

There are, in fact, other sources contributing to the fluctuations not included in formula (4) like the flicker $1/f$-noise (which is $\sim (C_{det}+C_{preamp})$ and independent on the time constant), the so called Johnson-noise ($\sim \tau/R_{APD}$, with $R_(APD)$ being the APD series resistance here assumed to be large) and the parallel f-noise (which reflects dielectric losses). Here we do not consider them as important for several reasons[5] which are confirmed by measurements of the RMD APDs even for rather long shaping time[4].

If we want to express the total signal fluctuations in Equivalent Noise Charge and exclude intrinsic Poisson fluctuations of incoming signal N_{signal}, then equation (4) becomes:

$$ENC^2 \approx (F-1)N_{signal} + F\frac{I_{bulk}\tau}{q} + \frac{I_{edge}\tau}{q}\frac{1}{M^2} + C_{APD}^2 \frac{4k_B T}{1.5 g_m q^2 \tau}\frac{1}{M^2} \tag{6}$$

[3]This formula is precise for ideal 'cusp' pulse shape but could be used also for semi-gaussian shaping as realistic approximation of this ideal case.

For our calculation we have taken the measured data on ENC for an existing $JFET$ preamplifier based on the transistor $KP340A$[6] and we have scaled it according to the simple ($\sim C^2_{APD}/\tau$) behaviour for the real APD capacitance and shaping time suitable for an ACT camera. This $JFET$ transistor can not be considered as the best possible choice (in fact we shall use, whenever possible, a transistor with capacitance matched to the capacitance of the selected APD) but nevertheless having capacitance C_{preamp} ≈5pF and C_{preamp}/g_m ≈0.2 nsec it is well adapted to the low capacitance and high parallel resistance RMD APDs.

The actual importance of each one of the terms in the above equations in order to cope with the goals of a future ACT camera design, will become clear in the results and discussions of the next sections.

3 The Excess Noise Factor (ENF) in APDs

Given the limited amplification per step in the impact ionisation mechanism responsible for the avalanche amplification in APDs, the subject of the excess noise factor was already addressed in detail when these devices were first developed. Two different kind of modelizations were developed to describe the ENF in APDs: first, a very simple and elegant approach in the limit of a continuous amplification process, due to McIntyre [7, 8] and afterwards a more realistic and complex one, assuming amplification in a discrete number of steps, due to K. M. Van Vliet[9]. It should be noted that the theory of McIntyre is in reasonable agreement with experimental data except at small ($M < 10$) gains. In that region, in which we are not particularly interested, the Van Vliet theory should be used.

To get a simple understanding of the origin of ENF in the APD amplification, it is useful to think in analogy to the amplification in the dynodes of a PM. Assuming that only the electrons do contribute to the ionisation amplification, the ENF is, in first approximation, a simple function of the amplification factor in each step m_i and the number of amplification steps N needed to get a given gain M[10]:

$$\begin{aligned} M &= m_1 m_2 m_3 \ldots m_N \\ F &= 1 + 1/m_1 + 1/(m_1 m_2) + \ldots + 1/(m_1 m_2 \ldots m_N) \end{aligned} \tag{7}$$

where, assuming now that each carrier will just produce in average a single electron-hole pair in each amplification step, then $m = 2$ and hence, for a large number of amplification steps, one would asymptotically expect:

$$F = 1 + 1/2 + 1/4 + \ldots \simeq 2 \tag{8}$$

This small step gain can be justified with the following argument: given the (large) typical ionisation potential ($\simeq 1.12$eV) in the avalanche region, and the large ionisation probability once this energy is reached, the incoming electron entering the avalanche region acquires just enough kinetic energy to produce one ionisation and then gets essentially stopped and has to start the process again. Therefore, if just the electrons do produce ionisation, each amplification step is then a $1 \rightarrow 2$ step with Poissonian probability.

This simple formulation should be qualitatively valid for low and moderate gains. Nevertheless at high gains (which may mean high electric field), which is the regime in which we are mainly interested, one of the basic underlying hypothesis in the above description is no more true: the ionisation due to holes may be not negligible and that has the direct effect of increasing the ENF due to the correlation between the electron and the hole amplification showers. In that situation, the excess noise factor F according to McIntyre's theory can be expressed as:

$$F = k_{eff}M + (2 - 1/M)(1 - k_{eff}), \tag{9}$$

where k_{eff} is the so called K-factor and, at very crude approximation, can be considered as the ratio from the average hole ionisation probability β_{hole} to the average electron ionisation probability α_{e^-}. Since M is large and k_{eff} should be as small as possible [3] the above formula reduces to approximately

$$F \simeq 2 + k_{eff}\,M \tag{10}$$

This is the expression which justifies the so-called MacIntyre's diagram: in first approximation, in the F v.s. M axes, the measurements lie on an

[3] In fact, symmetric expressions are obtained in the case that the main carriers participating in the avalanche are the holes instead of the electrons. Therefore, in general, the minimum of the excess noise factor is obtained either when k_{eff} is very large or when it is close to zero, being $k_{eff} = 1$ the worst case in what concerns ENF. In silicon, the main carriers responsible for the avalanche multiplication are the electrons and hence, the smaller the hole multiplication is, the better the performance of the device will be. To get small k_{eff}, special doping profiles or multi-layer techniques are used.

straight line of intercept 2 and slope k_{eff}. This diagram is used by all the companies to characterise the quality of their APDs and to determine their effective K-factor.

It is evident from (9) that even in the ideal case when only one type of carriers participate in the avalanche ($k_{eff} = 0$) the excess noise factor can not be less than two at high gain. That implies that, by no means, the signal from individual photoelectron can be resolved (see fig.1).

In fact, for the single photoelectron signal separation, the situation is even worse than what a simple-minded analysis of the above definition of ENF would predict: somehow, one naively expects the gain distribution to be a gaussian with the most probable value being the nominal average gain. In practice, for APDs this turns out to be a reasonably good approximation when the initial number of electrons to be amplified is above, say, 10 but it is far from being correct when it is just one or two. The basic reason is that, since the first step amplification is so poor ($1 \rightarrow 2$), the fluctuations on it modulate completely the gain. Figure 2 shows the expected gain distribution due to F for different initial number of photoelectrons. It can be seen that, in the case of just one photoelectron, the output charge distribution has an exponential-like falling shape. Therefore, no single photoelectron peak can be expected after the amplification even for very high gains.

One question which we would like to address here is whether the situation would improve if one would change the temperature. An increase in temperature is known to decrease sizeably the gain due to the fact that when the temperature of the semiconductor increases, the probability of diffusion of the free carriers over the crystal optical phonons increases. The energy losses of the free carriers increase and, hence, the electron and hole ionisation coefficients α_{e^-} and β_{hole} decrease leading to a decrease in the gain.

The relevant question is then whether, since α_{e^-} and β_{hole} will change with the temperature, one could predict a sizable change in the K-factor as well. Unfortunately, the actual absolute prediction of α_{e^-} and β_{hole} is a function of many parameters (such as, for instance, the applied electric field, the structure of the material (doping profile), crystal orientation, etc...) and therefore the answer to the above question is not straightforward.

At any rate, just to get a feeling, here we have used a simple parametrisation by Sze [11] of the "three-parameter" theory of Shokley, Wolf and Baraff to describe the diffusion of carriers with phonons[12]. We have seen qualitatively that these two ionisation coefficients will decrease in a rather similar way as the temperature increases(see figure 3). In fact, from that figure, if any tendency could be extracted at all for their ratio, it would be that in silicon k_{eff} would increase as the temperature decreases, degrading thus F beyond the degradation purely due to the change in the gain. That could be explained intuitively by the fact that, in silicon, the holes are somehow heavily "penalised" with respect to the electrons by their larger probability of scattering with phonons, which decreases their ionisation coefficient way below the one for electrons. Since the main effect of decreasing the temperature is reducing that scattering probability, it is somehow reasonable that the holes do "benefit" slightly more than the electrons and hence increase their ionisation probability slightly faster thus degrading k_{eff}.

Nevertheless, given the many simplifications assumed, the above discussion should be considered, if at all, only as qualitative until a more detailed modelling is used and/or experimental confirmation is obtained. So far we've not been able to find precise analyses in the literature. The detailed simulation and measurement of the behaviour of F as a function of the temperature is one of our projects for the near future.

Summarising: from all the above considerations our conclusion is that in "standard APDs" [6], we do not expect to see a single photoelectron peak and to be able to resolve individual photoelectrons. Nevertheless, some ideas about how to handle these limitations in the case of ACT cameras are just described in the next section.

4 Optimal gain and cooling for a realistic APD system

When we are talking about the implications of the use of APDs for low light level detection we shall consider two different classes of applications, in which it is necessary to use quite different detection techniques:

[6] APDs working in linear mode and designed to be able to operate at room temperature. At the end of this note we will describe few ideas on how this problem could be circumvented by using "non-standard" APDs.

4.1 Single photoelectron detection

In the first case, it is desirable to detect, if possible, every photon incident on the detector. In such an application it is necessary to minimise the pedestal width in order to separate as much as possible the pedestal from the single photoelectron response signal. Nevertheless, as we've just seen, for "standard APDs" the probability distribution of gains for small signals is highly non-Gaussian and can be quite reasonably parameterised in the framework of the semiconductor gain theory[13]. However, if the preamplifier ENC (pedestal width) is less than that of one photoelectron, then it is possible to detect single photons with detection probability better than the best available photomultiplier by just lowering the discriminator threshold setting.

Since there is no single-photoelectron peak, in such a case one is sensitive just to the right-hand side tail of single photoelectron spectrum. Nevertheless, since the APD quantum efficiency is very high, the detection probability for single photon will still be high too. Here one should not worry about the excess noise coming from the useful signal and one should just put more gain to overcome the electronic noise. Figure 4a shows that the optimum gain needed is quite high, but it is still lower than the maximum gain allowed for the RMD APDs.

It is clear from figure 4a that very small shaping times would be preferable as less leakage will be accumulated during the measurement. Cooling is essential and helps substantially in this case[7] especially for large surface APDs because it allows to reduce the APD dark current. Fig.4b shows that even for (10x10)mm^2 APDs, the requirements could be fulfilled at rather moderate cooling. Above certain gains, the increase of excess noise factor starts to be dominant and limits the system performance. It should be stressed here that for the above considerations we've assumed, by now, a negligible change of k_{eff} with the temperature.

[7] It is known that the bulk leakage current decreases by a factor of two for every 10^{o}C reduction in temperature. Although, as far as we know, this behaviour should still be confirmed for deep cooling (down to liquid nitrogen), we have still used the mentioned factor in our calculations.

4.2 Discrimination from night sky background

In the second class of applications, which is more close to the ACT requirements, it is desirable to discriminate against single-photon-induced events (night sky background in an ACT camera case) while at the same time detecting bunches of photons within a certain time duration with a high detection probability.

For example, the background from LONS (light of night sky) at La Palma in the $300 - 600nm$ optical band has been measured to be[14] $(1.7 \pm 0.4) \cdot 10^{12} photons/m^2 \cdot sr \cdot sec$. For a 200 m^2 collection mirror and APDs with $QE \sim 70 - 80\%$ and a preamplifier shaping time of $3nsec$ we will have about 3 photoelectrons per 0.1^o pixel as a mean value of a Poisson distribution.[8]

In the presence of some signal, like the natural background, we can not ignore the broadening of the spectra due to it (formula (6)). The ENC as function of gain for different levels of signal is presented on fig.5.

The role of cooling is not so prominent in such a case and the improvements by cooling tend to be saturated as can be seen in figure 6, where the signal-to-noise ratio versus gain is presented. Having a variance of the background close to 3, we should put the threshold for useful signal above 2-3 σ to reduce the cell counting rate up to an acceptable level. DC-level of background signals could be cancelled out by using AC coupling to the preamp electronic chain. There is no need in fact to discriminate between the bunches containing two and three or three and four etc. photons (photoelectrons) since, being deeply inside Poisson statistics at low level signals, we will anyway be, if not dominated at least largely influenced by its variance. It is desirable, however, to avoid as much as possible to disturb our measurements too much by additional fluctuations coming from the detecting system.

Let us consider 8 photoelectrons as a realistic value for the threshold setting in single cell.[9] The optimal gain for such signals will be even lower and the signal-to-noise ratio even a bit better as the two upper broken lines

[8]From Monte Carlo simulation results of the arrival time of photons to the camera cells, we've seen that 3 nsec integration time is somehow the lowest limit if we do not want to loose signal due to spread of arriving time of incoming photons.

[9]The real threshold will depend in particular on the DAQ rate capability and the acceptable dead time. Detailed calculations of the actual first-level trigger rate coming from LONS background that could be expected for different kind of photodetectors -PMs, HPDs and APDs- taking into account the actual QE and ENC expected for each device, have been carried out and will be the subject of a forecoming report.

in fig.7 demonstrate. As we see, the accessible signal-to-noise ratio could be considered as acceptable but still, the natural Poisson fluctuations will be raised by factor two.

Above, the most unpleasant case of large surface APDs has been considered. If we are able to concentrate the light to (5x5)mm^2 surface APDs using, for instance, high refractive index lightguides, we can gain a lot because of both: reduction in the APD capacitance and in the bulk dark current. This is shown by the two upper solid lines on fig.7.

Finally, one of the main questions is what can we expect if somehow (by "mysterious" technology development) the K-factor will be reduced, say, by a factor 10 ? This case is illustrated by the set of lower curves in the same fig.7 for two sizes of APD and for two different levels of signal.

5 Comparison between APD, PMT and Intevac HPD on trigger level

From the trigger point of view the most important criteria to choose the type of image camera photodetector are defined by the 1-st level trigger where we have to keep the threshold for useful signals as low as possible and, at the same time, trying to suppress the background rate up to an acceptable level for the DAQ. It is clear that, if all the other characteristics would be equal, the device with the highest QE will be preferable because of the features of Poisson statistics. In reality there is an interplay between different factors among which the most important ones are QE, ENF (which defines the broadening of the spectra) and ENC of the electronics chain. We do not consider timing assuming that all devices under consideration (and their amplifiers) may provide the 3 nsec time response needed. The parameters used for this study (along with some comments) are presented in the table 2.

The simulated spectra for different photodetectors (fig.8) agree with the ones observable in reality. In particular the PMT spectrum shows a single photoelectron peak with just a tiny indication of the second photoelectron. The HPDs allow more than that because of their extremely small ENF. All together proves that the parameters chosen for the analysis are reasonable. Note that spectra are ENC-normalised and take into account the QE of the photodetectors. So the 3 photons light bunches spectra correspond to background from LONS for all the photodetectors considered.

Extracted from these figures, the dependence of the "registration efficiency" on the threshold set, is shown in fig.9a. The curves marked as 3 photons bunch should be considered as the background suppression efficiency. Even more important, is the dependence of the registration efficiency versus the background suppression for different levels of signal, which is shown in fig.9b. One can see that up to factor 1000 in background suppression (what corresponds to about 300 kHz background rate in a single channel for a chosen time duration) the APDs give better signal registration efficiency than the PMTs. Further background suppression is limited by the nongaussian tails in the APD spectra discussed above. The same effect but with different physical origin takes place in the PMT system as well: due to afterpulses, the PMT 3 photons suppression curve presented on fig.9a as single exponent has in reality a second shoulder which defines the background rate[15]. In figure 9 we did not take this effect into account, although it clearly would make things much worse for PMTs (and maybe for HPDs) for large background suppression requirements. Nevertheless such afterpulses may affect the system performance even in the case of the Intevac HPD where special care has been taken at the design level to avoid it. If we believe that this effect is negligible for these devices the Intevac HPD is the best choice from the trigger point of view since the curves in fig.9b almost follow ideal Poisson features. It should be stressed, however, that having HPDs with the best ENF but with QE similar to usual PMTs we would bring the system performances down to the ones achievable in the APD case.

Nevertheless, keeping in mind the simple behaviour of the telescope threshold on the trigger and reconstruction level versus the QE (formulas 1-2), a conclusive comparison between the different photodetectors, should be done including also the "off-line" image analysis with the simulated response of the FADC system.

6 How to overcome the APD limitation to observe single photoelectrons?

As far as we know, at least two high-gain solid state photodetector concepts based on impact ionisation have proven to be able to resolve clearly single photoelectrons so far:

- On the one hand, the MRS (metal resistive surface) devices[16], in which the actual operation mode is not linear but "Geiger-like". The reason why, in spite of that, the signal from different number of photoelectrons can be resolved is that the device can be seen effectively as a large sample of individual micro-APDs with saturated gain connected in parallel. Since each photon is supposed to excite a different micro-APD, the signals add linearly. The main problem of such devices at present is that, by the technology used, the actual size of the "inneficient boundary" between the micro-APDs can not simply be controlled and, in fact, turns out to be very sizable, reducing thus drastically the effective quantum efficiency of the device below the limits that we are interested in.

- On the other hand, the VLPCs (visible light photon counters)[17], in which the operation mode is linear but have to operate at extremely low temperature (liquid Helium). The reason why these devices are able to circumvent McIntyre's limit is that, since they are aimed to work at very low temperature and then they have to cope with much smaller kT, the impurity concentration is such that the impact ionisation is designed to happen in the impurities ("impact ionisation of impurity-band electrons"), which present a very small band gap (about 50 meV), much smaller than that of normal APDs, for which the impact ionisation is supposed to happen in the silicon itself and hence has a gap of the order of 1.1 eV. In these conditions, the basic underlying assumption of McIntyre's theory is no more true: the electron originating the avalanche may make several ionisations before stopping, so that the first stage amplification becomes $1 \rightarrow N$ with N large instead of $1 \rightarrow 2$ which is the case in normal APDs. This immediately leads to an small ENF. Unfortunately, working at such low temperatures would be unpractical for an ACT camera.

Nevertheless, based upon these two devices, two modifications to the present standard APDs could be envisaged allowing to approach the single photon resolution limit:

- Following the concept of the MRS device, one could try to produce a sort of of fine-grain $(50x50)\mu m^2$ array of 40000 elementary standard APDs with a built-in parallel connexion as a single readout channel. That device should be operated in saturation (Geiger mode) in order to get a quasi-digital output per cell. That would allow a large enough sensitive area $(1x1)cm^2$ and it would be suitable for ACT cameras since then the probability of several photons going to the same channel would be small. One of the possible problem here is how much the "dead space" between APDs could be reduced this way and how good the performance of each individual APD channel could be kept.

- Following the concept of the VLPC device, one could try to see how much the concept could be pushed for an acceptably low temperature. If for the ACT camera a temperature of, say, -60^{o}C could be affordable, then one should take advantage of the decrease in kT to play with the use of the impurity band gap to allow a somewhat better first-stage amplification and hence an smaller ENF. Nevertheless, if this idea is at all possible, one possible caveat here is whether such limited decrease in temperature may be enough to allow a clear single photon resolution or not.

7 Conclusions

We have shown that, in spite of the inherent limitations of the standard APDs to resolve single photons in the high gain regime, they could still be used for ACT camera application in an effective way using the proper strategy. In addition, some hardware developments that could eventually help to reach the single photon resolution have been also discussed.

References

[1] The MAGIC Telescope. Proposal, 1998.

[2] Mirzoyan R., MAGIC Internal Note (?).

[3] Redus R. and Farrell R., SPIE International Symposium on Optical Science, Engineering and Instrumentation, July 1995.

[4] Farrell R. et al., SPIE International Symposium on Optical Science, Engineering and Instrumentation, July 1995.

[5] Radeka V., Ann. Rev. Nucl. Part. Sci. vol.**38**, (1989) 217.

[6] Guschin E., et al., CMS Technical Note CERN-CMS TN/93-108.

[7] McIntyre R.J., IEEE Trans. on Electron Dev., vol.**13**, no.1 (1966) 164.

[8] McIntyre R.J., IEEE Trans. on Electron Dev., vol.**19**, no.6 (1972) 703.

[9] Van Vliet K.M., IEEE Trans. on Electron Dev., vol.**26**, no.5 (1979) 752.

[10] See for instance, W.Shockley and J.R.Pierce, *A theory of noise for electron multipliers*, Proceedings of the IRE Vol 26, pp.321-332, 1938.

[11] Sze S.M., *Physics of Semiconductor Devices.* John Wiley & Sons, 1981.

[12] Capasso F., *Physics of avalanche photodiodes*, Semiconductors and semimetals, Vol.22, Part.D, pp.1-172, ATT Bell laboratories, Academic press, 1985.

[13] Conradi J., IEEE Trans. on Electron Dev., vol.**19**, no.6 (1972) 713.

[14] Lorenz E., Mirzoyan R., Preprint MPI-PhE/94-35, 1994.

[15] Lorenz E. et al., Proc. of the 1-st Conference on New Developments in Photodetecton, Beaune, France, June 24-28, 1996.
Hermann G. et all., Preprint MPI H-V36-1995, 1995.

[16] Akindinov A. et al., Nucl.Inst. and Methods **A**387 (1997) 231-234

[17] Petroff M. D. and Stapelbroek M. G, IEEE Trans. on Electron Dev., vol.**36**, no.1 (1989) 158.
Pettroff M. D. and Atac M., IEEE Trans. on Electron Dev., vol.**36**, no.1 (1989) 163.
Wayne M. R., Nucl.Inst. and Methods **A**387 (1997) 278-281.

[18] Blanchot J. et al., presented at IEEE Nuclear Science Symposium, Toronto, November 1998.

Breakdown Voltage, Volts	≈ 2000
Maximum Gain	≈ 10000
APD Area, mm^2	(1×1) to (16×16)
K-factor (k_{eff})	7.2×10^{-4}
Bulk Dark Current, pA/mm^2	≈ 4
Edge Dark Current (at Gain$\approx$3000), nA/mm	≈ 24
Capacitance, pF/mm^2	0.64
Parallel Resistance, GΩ·mm	> 100

Table 1: The parameters of RMD high gain APD at room temperature.

	APD	PMT	HPD
QE, %. Mean value (300-600)nm	70	10	40
ENF	Depends on gain (formula 9). Optimal gain (Capture 4) for low level signal and 3 photons as background in 3 nsec duration time does not exceed 1000.	1.2	1.025
Noise, ENC	See Capture 2	0.1 Defined by photocathode dark current and/or preamp noise.	0.3 Already achieved with a 300 Mhz bandwidth transimpedance amplifier[18].
Cooling	-60C^o saturates performances (Capture 4). Operation at room T reduces trigger efficiency at given background suppression by less than 10% as compare with fig.9b.	No.	No.

Table 2: The parameters for the analysis of the photodetectors at trigger level.

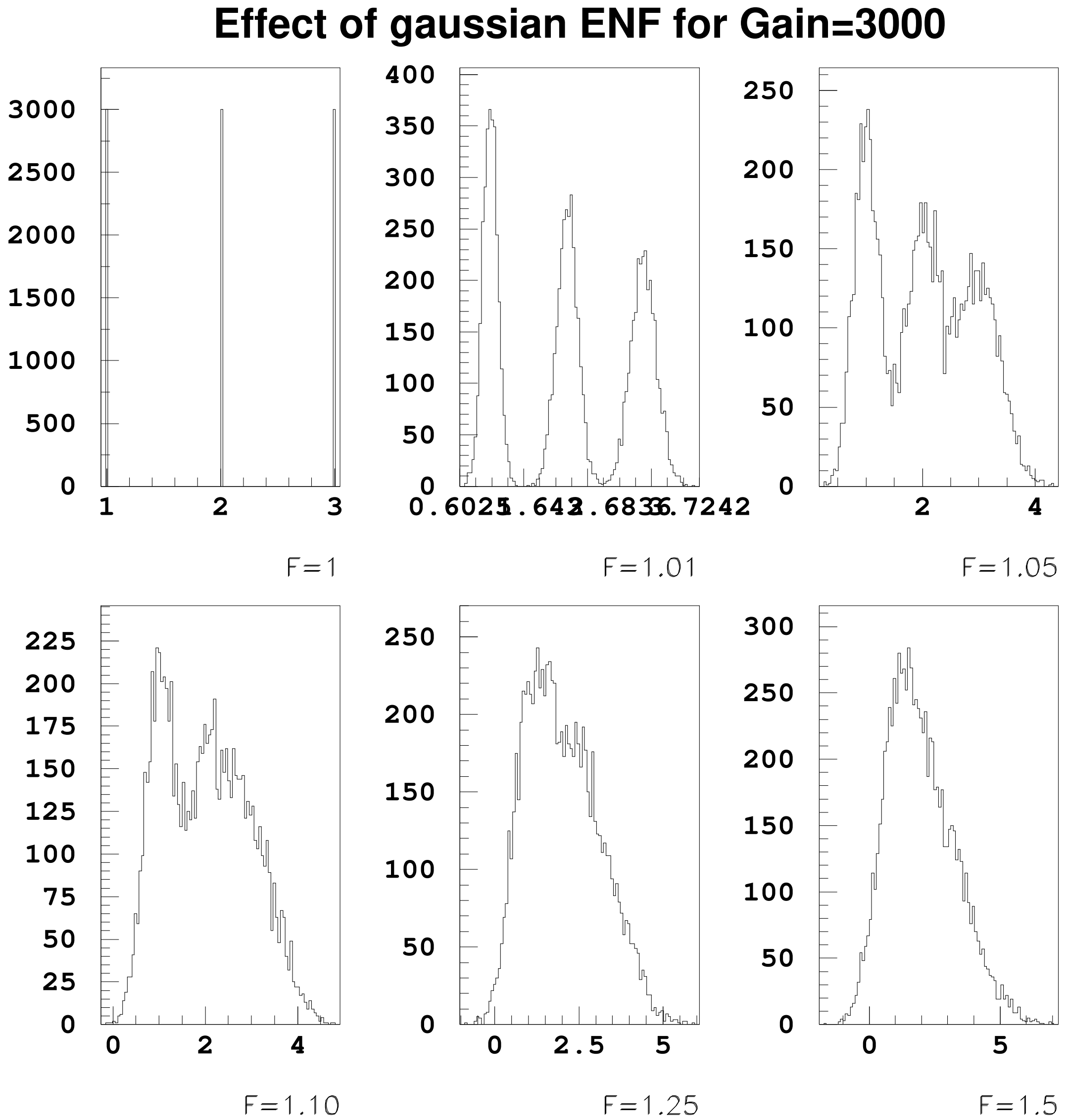

Figure 1: The separation between the peaks due to one, two and three photoelectrons for different values of the excess noise factor F. It is assumed that no other noise source is relevant and that the amplification procedure has a gaussian-shaped gain distribution (unrealistic for APDs but realistic for other photodetectors).

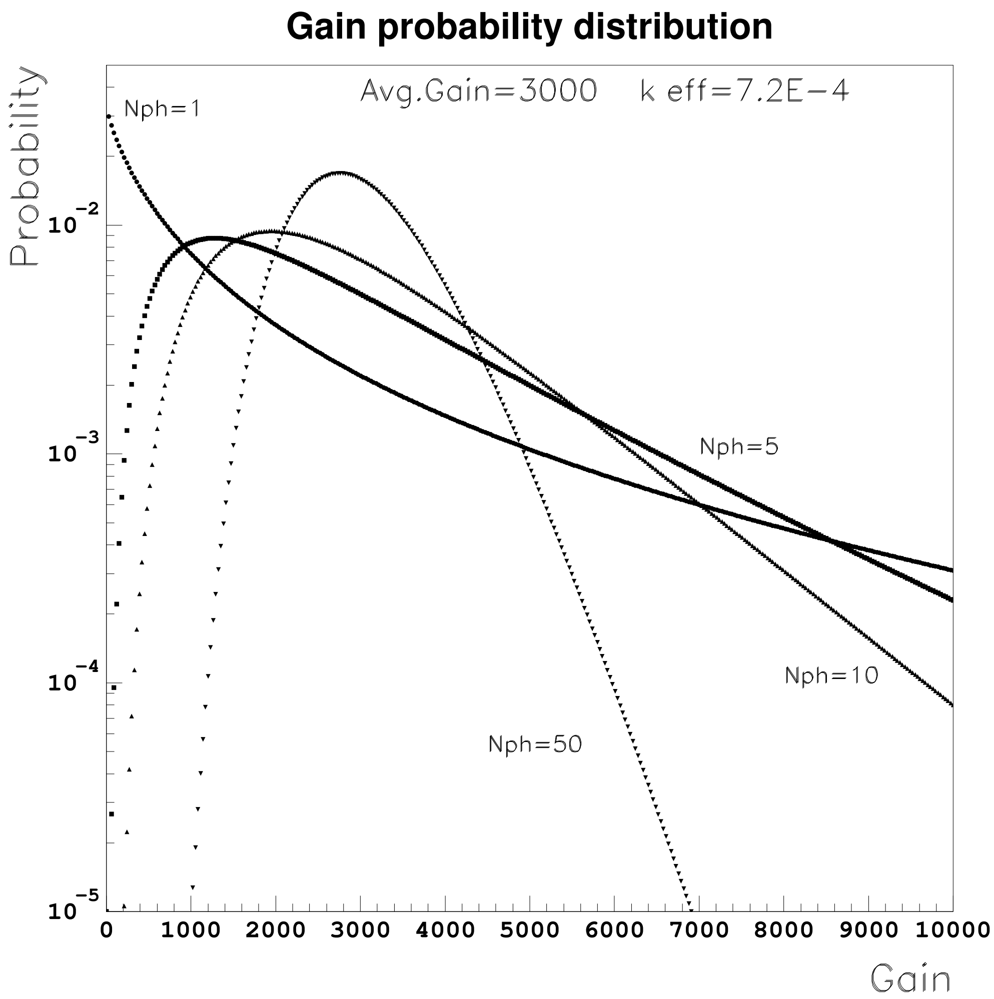

Figure 2: The actual expected APD gain distribution for different number of photoelectrons.

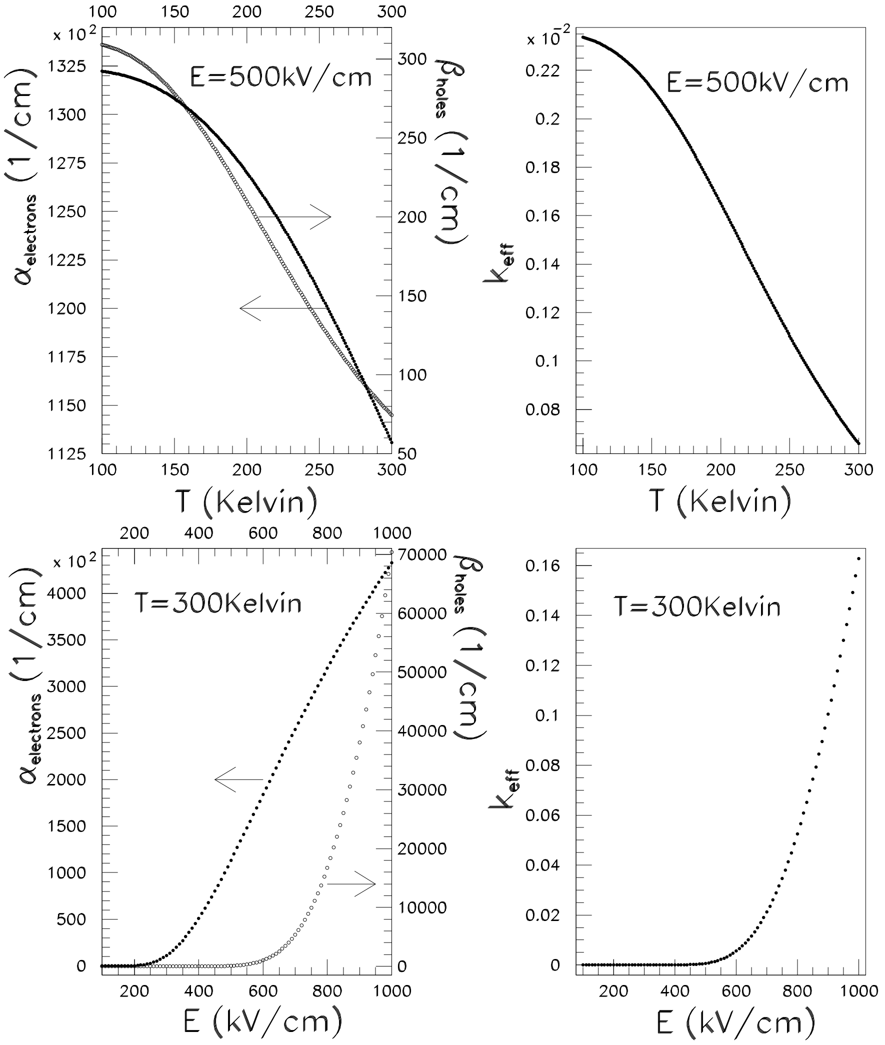

Figure 3: The expectation for the ionisation coefficients α_{e^-} and β_{hole} and their ratio k_{eff} for silicon as a function of the temperature and electric field. The parameters used are inspired in the RMD APD and the calculation uses the Sze parametrisation based on the "three-parameter" Baraff's theory (see text) and the k_{eff} claimed by RMD as an input.

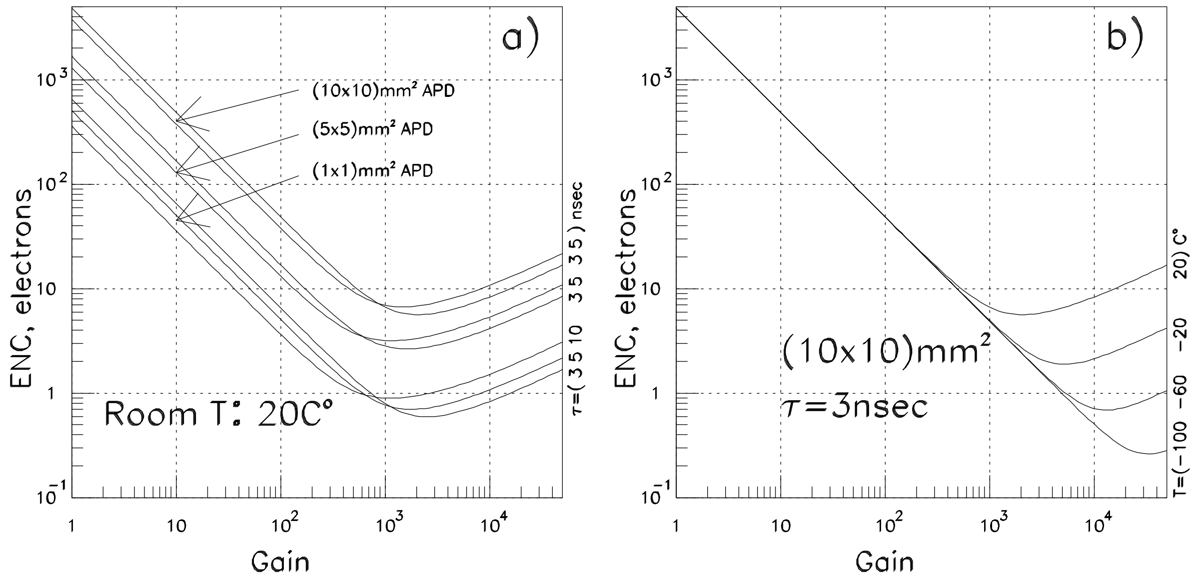

Figure 4: Equivalent Noise Charge of the APD+Preamplifier chain as function of APD gain in presence no signal.

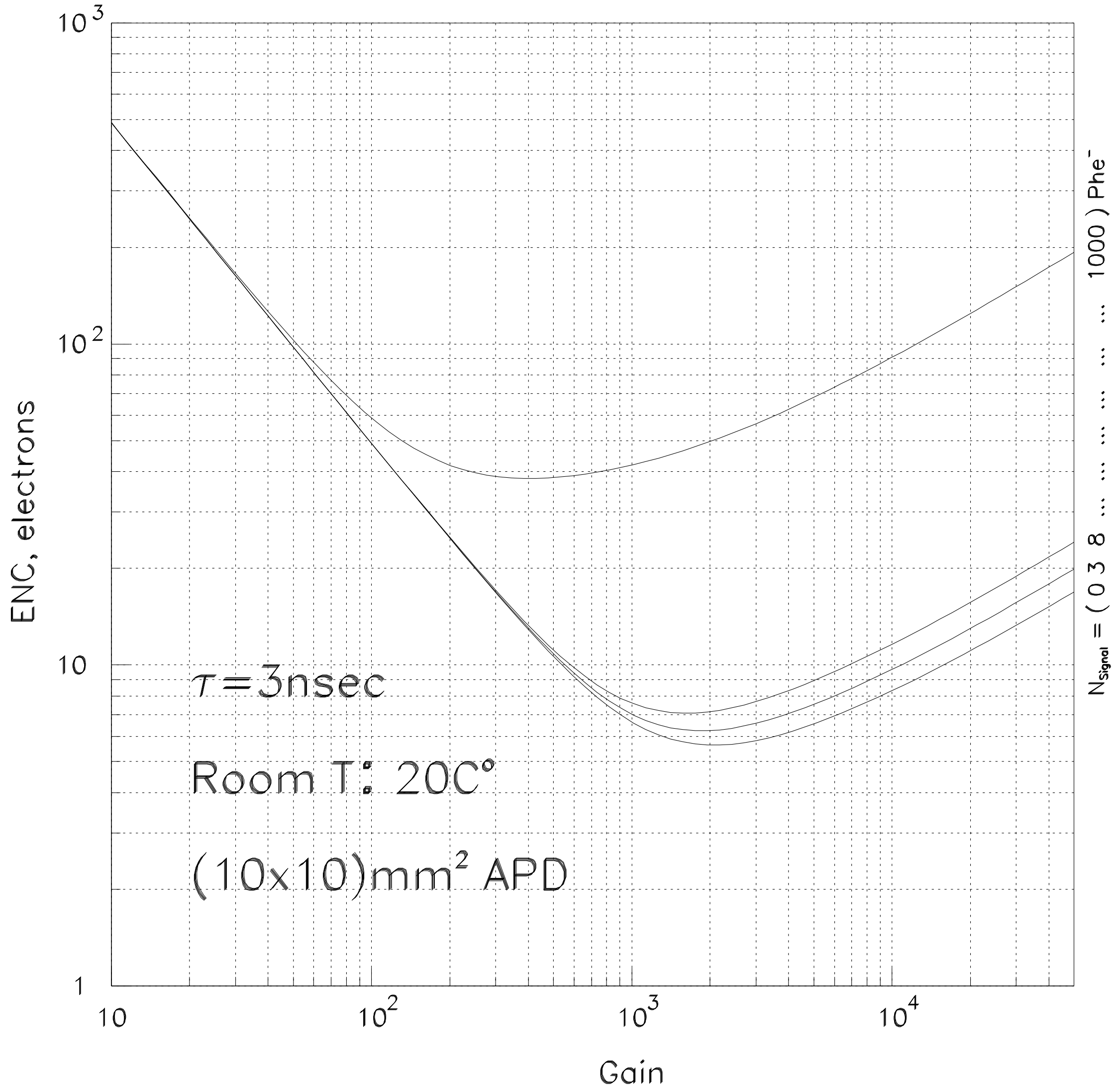

Figure 5: Equivalent Noise Charge of the detecting chain as function of APD gain for different signal levels.

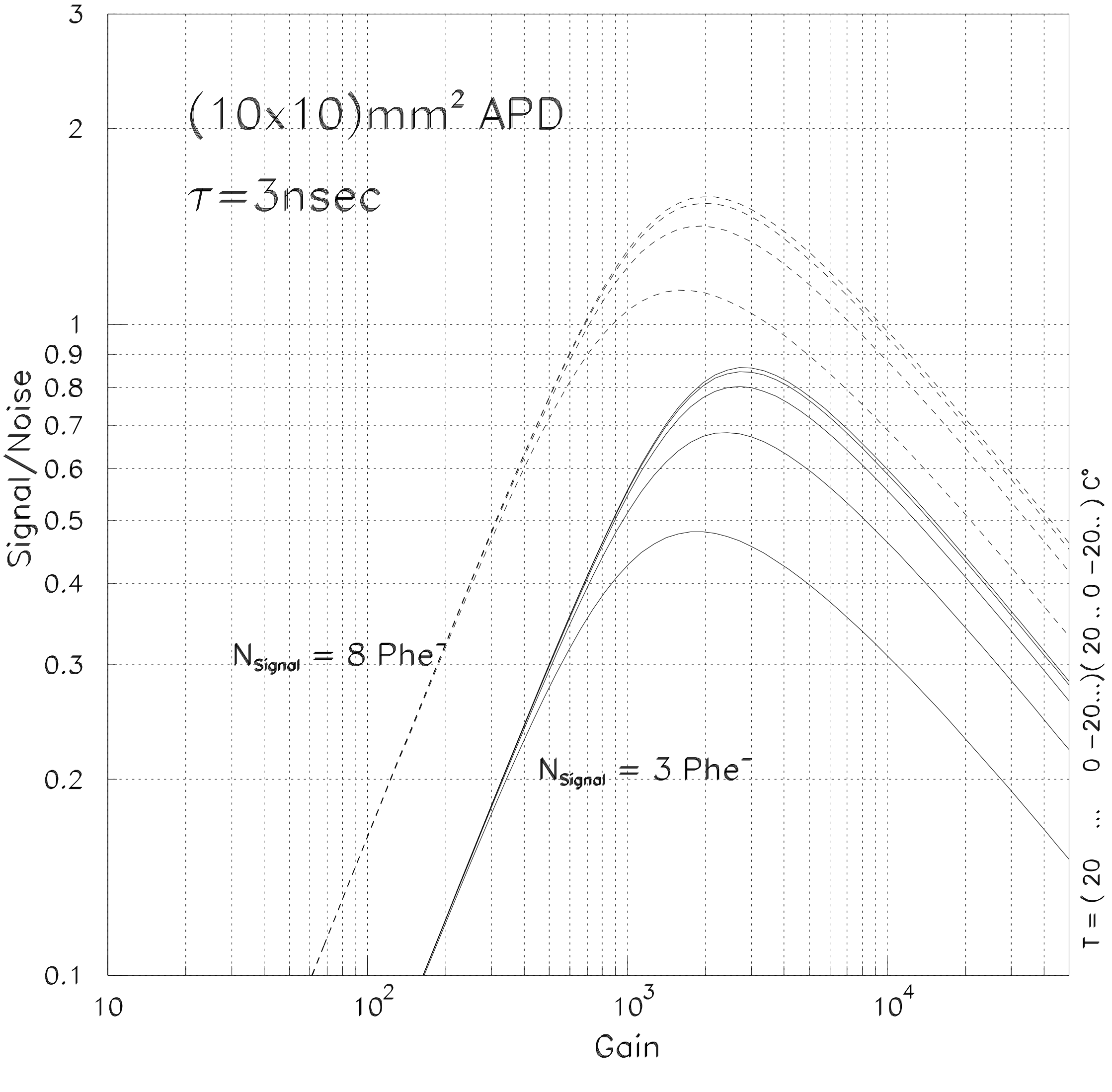

Figure 6: (Signal/Noise) ratio versus APD gain.

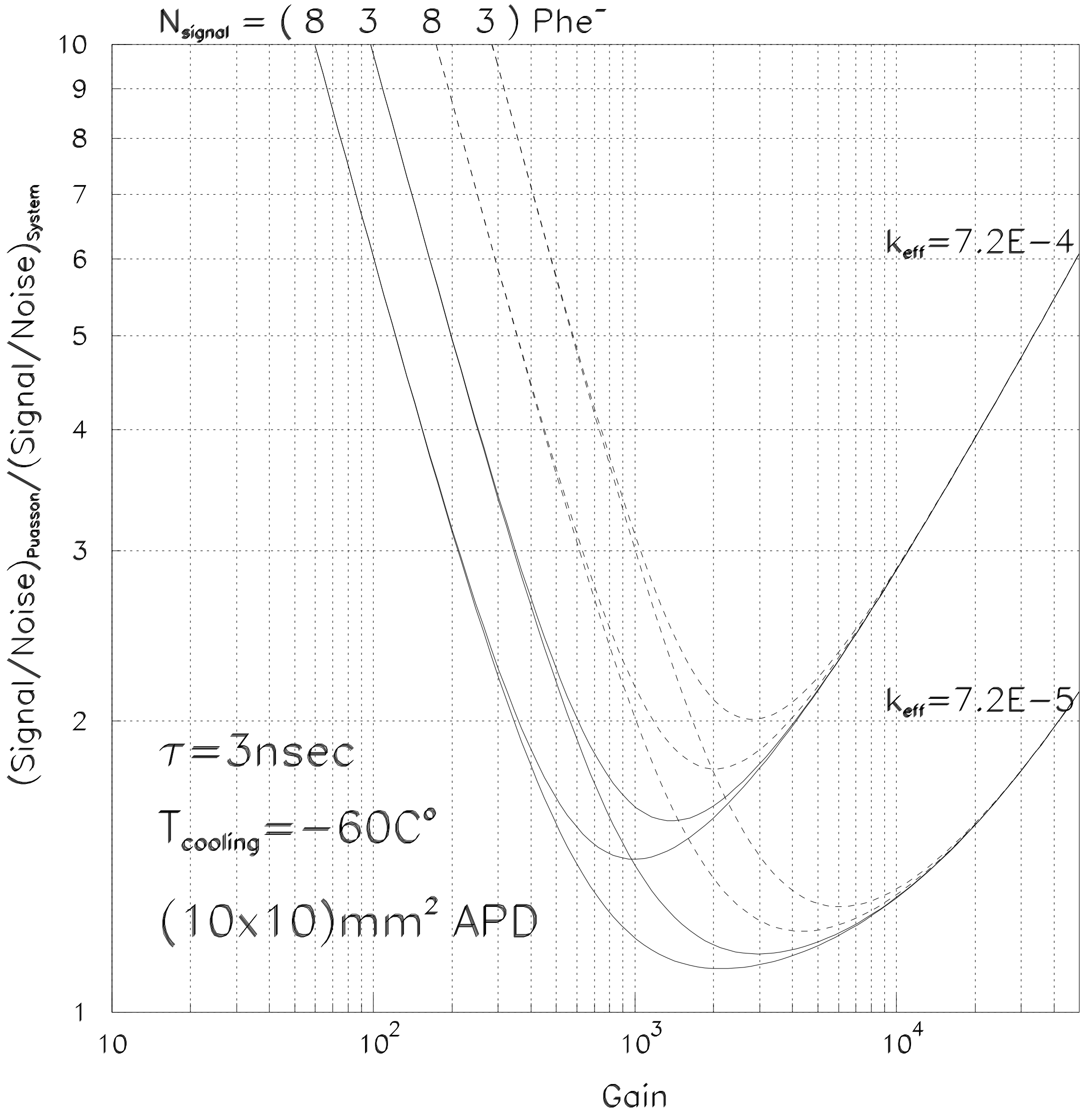

Figure 7: Ratio between (Signal/Noise) due to Poisson fluctuations and (Signal/Noise) due to detecting system versus APD gain for (5x5)mm^2 (solid line) and (10x10)mm^2 (broken line) surface APDs.

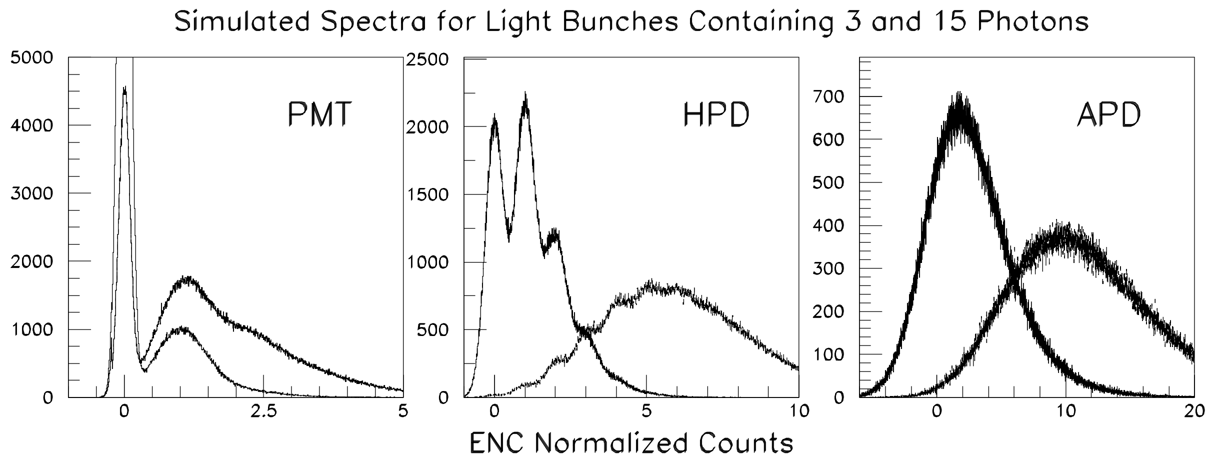

Figure 8: Simulated spectra for light bunches containing 3 and 15 photons.

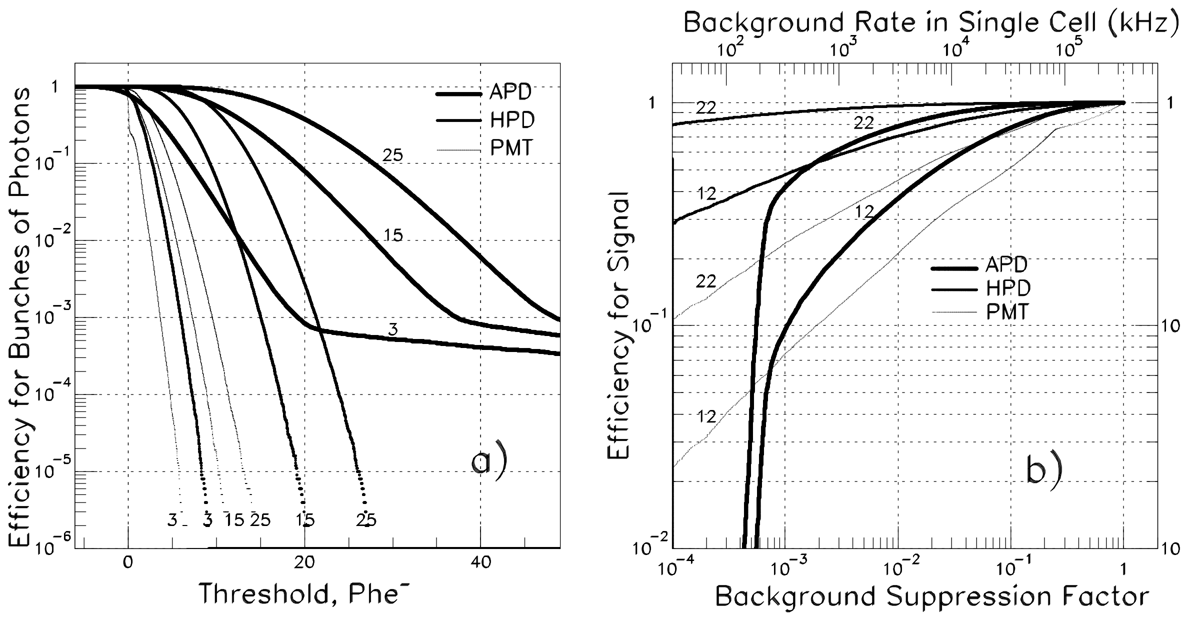

Figure 9: a). Registration efficiency versus threshold for different photodetectors and signal level (amount of photons in 3 nsec time duration are shown around the curves). b). Registration efficiency as function of background suppression/background rate in single channel. The digits around the curves show amount of photons in light bunches above the mean background level (see text for details).